Analyst

Accepted Manuscript

ROYAL SOCIETY OF CHEMISTRY

www.rsc.org/analyst

Ultrasensitive colorimetric assay of cadmium ion based on silver nanoparticles functionalized with 5-sulfosalicylic acid for wide practical applications

Weiwei Jin, Pengcheng Huang, Fangying Wu,* Li-Hua Ma*

Department of Chemistry, Nanchang University, Nanchang 330031, China

* Corresponding author: Fangying Wu, Tel: + 86 79183969882; Fax: + 86 79183969514; E-mail : fywu@ncu.edu.cn; Li-Hua Ma, Tel: 7134802039; Email: lihua2003@gmail.com.

Abstract

Low-level cadmium ion (Cd^{2+}) exposure contributes much toward the causation of chronic disease. Due to its low permissible exposure limit, overexposures may occur even in situations where trace quantities of Cd^{2+} exist. Until now, no effective treatment for Cd^{2+} toxicity has been reported. Prevention of further exposure is the most important step in management of patients suggestive of Cd^{2+} intoxication. Development of sensors for Cd^{2+} is of great interest to ensure early diagnosis and improve management. We propose here a simple, low-cost (0.1 $ per sample) yet very sensitive (limit of detection is 3.0 nM) and selective colorimetric assay for rapid (2 min) determination of Cd^{2+} based on 5-sulfosalicylic acid functionalized silver nanoparticles (SAA-AgNPs). This method exhibits excellent selectivity for Cd^{2+} over the other 16 metal ions. It is also precise and highly reproducible in determining Cd^{2+} in real samples such as tap water, milk, serum, and urine with recoveries ranging from 93 to 110%, indicating the wide practical applications to samples suspected of Cd^{2+} exposure.

Introduction

Cadmium ion (Cd^{2+}) is considered as a widespread health hazardous global pollutant. Although Cd^{2+} was banned in electrical and electronic equipment by the European Union's Restriction on Hazardous Substances,[1] the levels of Cd^{2+} still have increased recently in many areas due to human activities such as mining, smelting and fossil fuel combustion.[2] The resulting high Cd^{2+} contamination in soil, water and food has attracted great concern. Cadmium and solutions of its compounds are extremely toxic even in low concentrations. It can enter the food chain, bio-accumulate in organisms and ecosystems with a long biological half-life (about 30 years)[3] and therefore induces a wide variety of acute and chronic effects on human health.[4-6] Biological effects of chronic cadmium exposure include renal dysfunction, calcium metabolism disorders and an increase of certain forms of cancer, possibly due to direct inhibition of DNA mismatch repair by cadmium.[7] Health agencies such as the US environmental protection agency (EPA) have regulated exposure standards designed to protect the general public. For example, an estimate of a daily Cd^{2+} exposure to the general population that is likely to be without appreciable risk of deleterious effects during a lifetime for food and water is 0.001 mg/kg/day and 0.0005 mg/kg/day, respectively.

Scientists have been dedicated to develop facile assays of Cd^{2+} for the purpose of public health. The well-defined and generally accepted analytical techniques for measuring Cd^{2+} concentrations in biological samples are atomic absorption spectroscopy (AAS)[8] and inductively coupled plasma atomic emission spectroscopy (ICP/AES).[9] Roberts et al also reported to use graphite furnace atomic absorption spectroscopy (GFAAS) facilitated by a wet ashing pretreatment of samples to measure Cd^{2+} in blood and plasma.[10] It is apparent that these methods are inconvenient due to the complicated sample preparation and expensive sophisticated instrumentation. To date, a large number of colorimetric probes for metal ions have been developed.[11-13] Colorimetric-method-based nanoparticles seem to be a promising alternative for metal ions detection because of its appealing advantages including results visualization, high sensitivity, low cost and easy operation.[14-16] Gold nanoparticles (AuNPs) and silver nanoparticles (AgNPs) have become highly studied materials and been widely used due to their excellent optical and electrical properties.[17-21] One feature that makes them particularly outstanding is that AuNPs and AgNPs possess high extinction coefficients in the visible region. The colors of the dispersed and aggregated nanoparticles solution are different.[22] In addition, an introduction of ligands onto the surface of the metal nanoparticles can improve not only its water solubility but also the selectivity. Among these existing reports, colorimetric assays of Cd^{2+} based on Au or Ag nanoparticles have attracted extensive attention. Wang et al[23] developed 4-amino-3-hydrazino-5-mercapto-1,2,4-triazol single molecular functionalized gold nanoparticles (AuNPs) to sense Cd^{2+}, but Pb^{2+}, Ni^{2+}, Zn^{2+} and Hg^{2+} showed similar responses. Merkoci et al[24] reported a novel lateral flow immunosensor device for Cd^{2+} determination in drinking and tap water using Cd-EDTA-BSA-AuNPs conjugated as signal producer with 0.1 ppb detection limit. But as far as real sample analysis was concerned, the metal interferences had to be masked by sample pretreatment, which increased the detection time and labor. Most recently, Guo et al[25] reported a novel method for Cd^{2+} based on label free AuNPs with the aid of high salt concentration and glutathione. The LOD of this simple method is 5 μM, and Pb^{2+} obviously shows response to this system. Anthony et al[26] demonstrated the N-(2-hydroxybenzyl)-valine and N-(2-hydroxybenzyl)-isoleucine organic ligands modified AgNPs to detect Cd^{2+}, Pb^{2+} and Hg^{2+} at ppm level. Zhang et al[27] also developed the peptide-modified AuNPs for parallel detection of Cd^{2+}, Ni^{2+} and Co^{2+}. Specific chemicals such as EDTA and imidazole were applied to mask Ni^{2+} and

Co^{2+} for the purpose of Cd^{2+} determination. Li et al[28] reported a colorimetric sensing for Cd^{2+} using triazole-ester modified AgNPs with LOD as 20 μM. It has to be pointed out that the triazole ester was not commercially available and had to be synthesized based on 4-(prop-2-ynyloxy)pyridine in this method. Therefore establishing methods to detect Cd^{2+} sensitively and selectively is still demanding, particularly for the purpose of real samples analysis.

5-Sulfosalicylic acid dehydrate is a stable and non-toxic ligand, which bears three potential coordinating groups: –OH, $–CO_2H$ and $–SO_3H$. Therefore, it can coordinate to metal ions in different modes[29], which means its selectivity is poor. Owing to the fact that the sulfonic group is easily bonded with AgNPs, we prepared the AgNPs capped with 5-Sulfosalicylic acid dehydrate (SAA-AgNPs) and explored its responses to heavy metal ions. The results showed that only Cd^{2+} induced the immediate SAA-Ag-NPs aggregation, leading to a simple and rapid platform for the specific detection of Cd^{2+}. The detection limit of this cheap colorimetric assay is 3.0 nM, which makes the proposed assay one of the most sensitive colorimetric sensors among the metal nanoparticle-based methods. The proposed mechanism is depicted in Scheme 1.

(Scheme 1)

Experimental section

Materials

All chemicals were of analytical reagent grade and used without further purification. Silver nitrate ($AgNO_3$), sodium borohydride ($NaBH_4$), 5-Sulfosalicylic acid dehydrate (SAA) and the metallic ions were purchased from Shanghai Qingxi Technology Co., Ltd. (Shanghai, China, www.ce-r.cn/sites/qingxi/). BSA (bovine serum albumin), UA (uric acid), HSA (human serum albumin) and CS (casein) were purchased from Shanghai Sangon Biotech Co Ltd. (Shanghai, China, www.sangon.com/sangonindex.aspx). The distilled water used was purified through a Millipore system. Since cadmium is a ubiquitous element, the risk of contamination during sampling, processing and analysis must be minimized by strict laboratory procedures. All the glassware used must thoroughly be washed with freshly prepared aqua regia (3:1; HCl/HNO_3) and then rinsed comprehensively with ultrapure water and air dried prior to use.

Synthesis of SSA-AgNPs

The AgNPs were prepared according to the previously reported method[30] in which the $AgNO_3$ was reduced to Ag using $NaBH_4$. Briefly, in a flask, 2.0 mL of 0.01 M $AgNO_3$ was added into 97 mL doubly distilled water. Then 8.8 mg of $NaBH_4$ was quickly added into above mixture solution under vigorous stirring for 30 min at room temperature (25 ± 2 ºC), 1.0 mL of 0.01 M SAA was then added into the above aqueous solution. The resulting yellow silver colloidal solution was stirred for 2 hours in the dark room. Finally, the as-prepared silver colloidal solution was stored at 4 ºC in the dark before use.

Characterization of SAA-AgNPs

The formation of SAA-AgNPs was preliminarily characterized by visual observation of the bright yellow color of the solution and further confirmed by the UV-vis spectra acquired by UV-vis 2550 spectrometer (Shimadzu, Kyoto, Japan) using a 1.0cm quartz cell. A sharp peak at 390 nm is the typical absorption of AgNPs. The obtained solution was centrifuged at 8000 rpm and the bright yellow SAA-AgNPs precipitate was collected and placed in a vacuum dryer (DZF-6030A) for 12 hours at 40 ^{o}C and 133 pa. The dried materials were subjected to Nicolet 380 FTIR analysis in KBr pellets in the range of 400-4000 cm^{-1}. Transmission Electron Microscopy (TEM, JEOL-2010, operating at 200 kV) technique was utilized to determine the size and shape of the nanoparticles. The samples were prepared by drop-coating 20 μL SAA-AgNPs solution onto a carbon-coated copper grid (3 mm, 300 mesh).

Colorimetric detection of Cd^{2+}

A 1.0×10^{-4} M aqueous solution of Cd^{2+} was prepared. In a typical experiment, 2 mL of SAA-AgNPs (6.5 nM, which was calculated based on a previous report[31]) was mixed with different amounts of Cd^{2+} solutions to give final Cd^{2+} concentrations in the range of 0 to 1.1 μM. Finally, the color changes were detected by the naked eye and/or by UV-vis absorption spectra. The photographs were taken with a digital camera, and the UV-Vis spectra were recorded between 300 nm and 800 nm. The extinction ratio at 540 and 390 nm (A_{540nm}/A_{390nm}) has been used as the index parameter of SAA-AgNPs for detection of Cd^{2+} because the numerator and the denominator represent the degree of dispersion and aggregation, respectively. All the experiments were performed in triplicate. Limit of detection (LOD) values was calculated using the following

equation: LOD = 3 S_0/K, where S_0 is the standard deviation of blank measurements (n = 10) and K is the slope of calibration line.

Recovery experiments in tap water, lake water, milk, urine and serum

The detailed pretreatment for real samples (such as tap water, lake water, milk, serum and urine) was presented in Supporting Information. Recovery experiments were performed under the above-mentioned conditions, in which the pretreated samples were spiked with different concentrations of Cd^{2+}. The absorption spectra of the SAA-AgNPs sensor were recorded accordingly. Based on the established calibration equation of the ratio A_{540nm}/A_{390nm} versus Cd^{2+} concentrations in the section above, the found concentrations of Cd^{2+} spiked in the samples were calculated. And then, the recovery values for the samples were obtained using the following equation,

$$\text{Recovery (\%)} = (\text{calculated } Cd^{2+}/\text{spiked } Cd^{2+}) \times 100\%$$

Results and discussion

Characterization of SAA-AgNPs

The formation of SAA-AgNPs was estimated by the color change of the solution. It could be seen that the color of the reaction solution gradually turned yellow from colorless; the latter was initial color of $AgNO_3$ aqueous solution. UV-vis absorption spectrum of the resulting AgNPs showed a typical surface plasmon resonance absorption peak at 390 nm (Fig. 1A, black line), indicating that AgNPs exhibited good dispersibility, which was also confirmed by the corresponding TEM image (Fig. 1B-a). In addition, from their size distribution according to TEM image (Fig. S1, Supporting Information), we calculated that the mean size of SAA-AgNPs is 8.24 nm.

(Fig. 1)

FTIR spectra for SSA and SAA-AgNPs were shown in Fig. 2. For pure SAA, the bands of 1170-1281 cm^{-1} were the characteristic stretching vibrations of sulfonic group, and the peak at about 1674 cm^{-1} was assigned to the stretching band of carboxyl group. For SAA-AgNPs, the typical bands of sulfonic group in SAA reduced remarkably or almost disappeared, while the band

of carboxyl group still existed, although the peak slightly shifted (to 1653 cm^{-1}). These results indicated that SAA had successfully been bound onto the surface of the AgNPs via the sulfonic group of SAA.

(Fig. 2)

Mechanistic investigation on colorimetric assay of Cd^{2+}

Fig. 1 showed the absorption spectra (Fig. 1A), color changes (Inset of Fig. 1A), and TEM images (Fig. 1B) of SAA-AgNPs aqueous solution in the absence and presence of Cd^{2+}. For the initially well-dispersed AgNPs, upon the addition of Cd^{2+} (0.7 μM), the absorbance at 390 nm decreased sharply and a new absorption band at 540 nm appeared obviously. Meanwhile, the color immediately changed from bright yellow to red. Above changes were considered to be attributed to the aggregation of SAA-AgNPs, which was also observed by TEM images. To verify that the aggregation of AgNPs was not induced by salt effect, we added NaCl (0.7 mM) into AgNPs solution; note that this concentration was much higher than that of Cd^{2+}. We found that both the color and the UV-vis spectrum of the AgNPs solution remained almost unchangeable compared with those without NaCl. This result substantially ruled out the possibility of the salt-induced aggregation of AgNPs, further demonstrating that the changes observed in Figure 1A (vial b, red line) were essentially induced by Cd^{2+}. This phenomenon was elucidated by the coordination interaction between Cd^{2+} and SAA on the surface of the AgNPs; the O atom in the hydroxyl group and the O atom in the carboxyl group of SAA coordinated to Cd^{2+}, forming a stable complex by providing lone pairs into empty orbitals of Cd^{2+} and creating dipolar bonds (Scheme 1).[32-34] Such a surface coordination interaction eventually led to the aggregation of AgNPs, being responsible for the changes in both the color and the UV-vis spectrum of SAA-AgNPs aqueous solution. Strong coordination interaction between Cd^{2+} and SAA contributing to the aggregation of SAA-AgNPs could also be easily confirmed by excessive addition of a powerful chelating agent, ethylenediaminetetraacetic acid (EDTA) (1 mM), into the Cd^{2+}-triggered aggregated AgNPs solution. As depicted in Fig. S2, the presence of EDTA recovered the absorption spectrum of SAA-AgNPs almost to the original state, also indicating good producible manner of the sensor.

(Scheme 1)

Optimization of the Sensing Conditions

Following the design strategy, the performance of the developed method for Cd^{2+} is strongly influenced by the sensor SAA-AgNPs. Different sensing conditions, including pH effect, the molar ratio of AgNPs and SAA, and incubation time, were investigated in our study. The pH value of the as-prepared SAA-AgNPs was 9.5. The value of pH higher than 10 is not beneficial since Cd^{2+} may react with OH^- to form the corresponding metal hydroxides, which would affect the accuracy to some extent. Based on these considerations, the pH investigation was focused on the range from 4 to 10. It was found that pH had not much effect on the response of SAA-AgNPs toward Cd^{2+}, therefore, pH 9.5, which was the pH of as-prepared SAA-AgNPs solution without any pH adjustment, was selected. The molar ratio of AgNPs and SAA was found to be an important factor to affect the intensity ratio (A_{540nm}/A_{390nm}) as shown in Fig. 3A. It was observed that the intensity ratio increased with increasing the SAA concentrations in the molar ratio of AgNPs and SAA from 2:1 to 1:1, and exhibited a decrease when the ratio was 1:2. Considering that the concentration ratio of 1:1 had more dissociative SAA and, the ratio of 1:1 and 2:1 had small distinction, synthesis ratio of 2:1 was selected. Fast response time at room temperature is a key feature of an excellent sensor since it is highly preferred for on-site and real-time detection of Cd^{2+}, so we investigated the aggregation kinetics of the sensor with different concentrations of Cd^{2+} (0.3, 0.5, 0.6, 0.7, and 0.8 μM) by monitoring the value A_{540nm}/A_{390nm} of the SAA-AgNPs solution at room temperature. As shown in Fig. 3B, once Cd^{2+} was added, the absorbance extinction ratio increased rapidly and reached a relatively constant value in 2 minutes, which was in good agreement with the color change observed by visual inspection, revealing that the aggregation of SAA-AgNPs was able to be completed within 2 minutes under this condition. Such fast response of this assay makes it particularly suitable for on-site and real-time Cd^{2+} monitoring. Thus, pH, the molar ratio of AgNPs and SAA, and incubation time were optimized for the assay to be 9.5, 2:1, and 2 minutes, respectively. It should be noted that SAA-AgNPs showed high stability when upon the addition of Cd^{2+} at 25 ºC for 5 h and stored at 4 ºC in the dark for 18 days, respectively (Fig. S3).

(Fig. 3)

Selectivity of the assay

To study the recognition ability of SAA-AgNPs, the responses of a variety of metal ions (0.7 μM), such as Cd^{2+}, Al^{3+}, Ba^{2+}, Ca^{2+}, Cu^{2+}, Ag^{+}, Co^{2+}, Cr^{3+}, Fe^{3+}, Mg^{2+}, Hg^{2+}, K^{+}, Mn^{2+}, NH_4^{+}, Zn^{2+}, Ni^{2+}, and Pb^{2+} to SAA-AgNPs were investigated and shown in Fig. 4 (blue bar) and Fig. S4A. All the detections were carried out under the optimal conditions. It was revealed that the other metal ions had no obvious effect on the UV-vis absorption of SAA-AgNPs and almost no absorption changes were obtained, indicating that the absorbance ratio enhancement effect on the SAA-AgNPs was specific to Cd^{2+}, implying excellent selectivity of this strategy for Cd^{2+} detection.

It has to be pointed out that free SAA showed the responses to metal ions (Fig. S4B). But after it reacted with the AgNPs, only Cd^{2+} showed unique changes. For that the ligand shows selectivity change after anchoring on the surface of AgNPs, although it remains difficult for us to provide solid evidence to elucidate this interesting phenomenon, we speculate that it could possibly be attributed to changes from both binding sites of SAA and the pH of the solution after anchoring on the surface of AgNPs. As demonstrated by FTIR in Fig. 2, the SO_3^{-} groups of SAA were bound onto the surface of the AgNPs. For Ag^{+}, because Ag^{+} could coordinate to carboxylic, hydroxyl, and sulfonic groups of SAA,[35] its affinity with SAA weakened after AgNPs formed. For Fe^{3+}, it could interact with carboxylic and hydroxyl groups of SAA at low pH; aqueous solution of free SAA was acidic. Whereas, the pH of the SSA-AgNPs colloidal solution was 9.5 after SAA-AgNPs formed, in which Fe^{3+} easily underwent hydrolysis to produce Fe(III) hydroxides,[36] resulting in the inhibition of coordination interaction between Fe^{3+} and SAA. For other metal ions mainly coordinating to SAA through carboxylic and hydroxyl groups, the two above-mentioned factors might have a synergistic effect on their binding strengths with SAA, eventually leading to good selectivity toward Cd^{2+}. It has to be admitted that detailed investigations should further be going on for this selectivity change.

Interference analysis was performed to Cd^{2+} that was evaluated in the mixture of cationic, anionic ions, biological species, and surfactants solution that might interfere with Cd^{2+} detection in real samples. The presence of following amounts of foreign species compared with the concentration of Cd^{2+} resulted in less than ± 10% error: 1000 times the concentration of NO_2^{-}, Na^{+}, 100 times the concentration of K^{+}, NH_4^{+}, Ca^{2+}, Mg^{2+}, CO_3^{2-}, 50 times the concentration of Ba^{2+}, HPO_4^{2-}, 20 times the concentration of Hg^{2+}, 10 times the concentration of Al^{3+}, Co^{2+}, Ni^{2+}, Ag^{+}, Zn^{2+}, SO_3^{2-} and S^{2-}, 5 times the concentration of Cu^{2+}, Fe^{3+}, I^{-}, 1 time of Cr^{3+}, Mn^{2+} and Pb^{2+}, 100

times the concentration of glucose, 10 times the concentration of UA, 45 ppm of BSA and CS, 5 ppm of HSA. Meanwhile, the effect of surfactants was also inspected. The existence of 500 times of non-ionic surfactant (polyoxyethylenenonylphenol ether, OP-emulsifier) and anionic surfactant (sodium dodecyl sulfate, SDS) didn't interfere. However, 1 time of cationic surfactant (cetyltrimethylammonium bromide, CTAB) interfered with the determination of Cd^{2+}, presumably due to the feature of SAA-AgNPs with negative charges. These results showed that the sensor had good selectivity toward Cd^{2+} against other metal ions, anions, and biological species.

(Fig. 4)

Sensitivity of the Assay

Analytical detection performance of the proposed sensing system for Cd^{2+} was evaluated under the optimum conditions, the SPR peak shift of SAA-AgNPs was monitored by the UV-vis spectroscopy, and the extinction ratio between 540 nm and 390 nm was compared at various Cd^{2+} concentrations. As shown in Fig. 5, the intensity ratio A_{540nm}/A_{390nm} shows a linear response toward Cd^{2+} within a concentration range from 0.05 to 1.1 μM (A_{540nm}/A_{390nm} = 0.2624 + 0.056 $C/10^{-7}$ M, R = 0.9936). The limit of detection was 3.0 nM, calculated from S/N = 3, which was much lower than the maximum contaminant level of Cd^{2+} (45 nM) in drinking water by United States Environmental Protection Agency (EPA). Most of the reported assay can't meet the requirement by EPA. For example, thin film Cd^{2+} chemosensor (1 μM),[37] laser induced breakdown spectroscopy (4.5 *m*M), quantum dot-based turn-on fluorescent probe (0.5 μM),[6] triazole-ester modified silver nanoparticles colorimetric sensing (25 μM),[28] gold nanoparticles colorimetric method (30 nM[23] and 5 μM[25]) , and atomic absorption spectrometry (AAS, 27 nM).[8] This method is comparable to the value reported by the atomic emission spectrometry (AES, 2 nM),[9] however, without the need of the expensive instrumentation and professional staffs. The detailed comparison is organized in Table S1.

(Fig. 5)

Practical Applications

To evaluate the applicability of the colorimetric assay to real samples, tap water, lake water, milk, urine and serum were spiked with Cd^{2+} and tested by the assay. The samples were firstly pretreated according to the procedures in Supporting Information. We found that SAA-AgNPs sensor responses in real samples were very similar to those in distilled water, suggesting that the colorimetric assay can detect Cd^{2+} without being affected by the environment (Fig. S5). In addition, recovery experiments using spiked real samples with 3 different concentrations of Cd^{2+} were performed and summarized in Table 1. Average recovery value of 99% was obtained, indicating that the colorimetric assay could be used for the detection of Cd^{2+} in real samples from different fields with high accuracy.

(Table 1)

Conclusions

In summary, a colorimetric sensor for the detection of toxic heavy metal Cd^{2+} using SAA-AgNPs with high sensitivity and selectivity was proposed. The presence of Cd^{2+} was able to induce the rapid aggregation of SAA-AgNPs through cooperative metal-ligand interaction between Cd^{2+} and SAA, resulting in color change that is easily observed by the naked eyes. It has to be pointed out that several metal ions such as Fe^{3+}, Al^{3+}, Cu^{2+}, and Ag^{+} have a similar response to Cd^{2+} if chelated to free SAA. However, by anchoring on the surface of AgNPs, SAA may be assembled to provide appropriate binding sites and coordination environment that are favored by Cd^{2+}, which eventually dramatically enhance the recognition compared with free SAA. The proposed low-cost and rapid-reaction method was successfully applied to determine Cd^{2+} in real samples such as tap water, milk, urine, serum with satisfactory recovery, which in turn confirms that the coexistence of some common ions, surfactants, biological species doesn't interfere with the assay, allowing the on-site screening of products suspected of the Cd^{2+} exposure with high reliability, repeatability and reproducibility. Our assay is advantageous over the published nanoparticle-based methods, not only the detection of limit but also the wide-field practical applications.

Acknowledgements

This work was financially supported by National Natural Science Foundation of China (No. 201365014), Jiangxi Province Science and Technology University Ground Plan Project (KJLD No. 14007) and Jiangxi Province Natural Science Foundation (JXNSF No. 20132BAB203011).

Notes and References

1 The European parliament and the council of the European Union, "Directive on the Restriction of the Use of Certain Hazardous Substances in Electrical and Electronic Equipment". 2002/95/EC.

2 R. L. Chaney, J. A. Ryan, Y.M.Li and S. L. Brown, Cadmium in soils and plants. Edited by M J Mclaughlin and B R Singh, Kluwer, Boston. 1999.

3 S. Haouem, N. Hmad, M. F. Najjar, A. E. Hani and R. Sakly, *Exp.Toxicol. Pathol.* 2007, **59**, 77.

4 G. F. Nordberg, R. F. M. Herber and L. Alessio, Oxford university press, Oxford, UK. 1992,**118**, 469.

5 H. N. Kim, W. X. Ren, J. S. Kim and J. Yoon, *Chem. Soc. Rev.*, 2012, **41**, 3210.

6 H. Xu, R. Miao, Z. Fang and X. H. Zhong, *Anal. Chim. Acta*, 2011, **687**, 82.

7 C. T. McMurray and J. A. Tainer, *Nat. Genet.*, 2003, **34**, 239.

8 G. Kaya and M. Yaman, *Talanta*, 2008, **75**, 1127.

9 A. C. Davis, C. P. Calloway Jr and B. T. Jones, *Talanta*, 2007, **71**, 1144.

10 C. A. Roberts and J. M. Clark, *Bull. Environ. Contam. Toxicol.*,1986, **36**, 496.

11 (a) Y. Lin, C. Huang and H. Chang, *Analyst*, 2011, **136**, 863. (b) Y. Wang, F. Yang and X. R. Yang, *ACS. Appl. Mater. Interfaces*, 2010, **2**, 339.

12 (a) J. W. Liu and Y. Lu, *Chem. Commun.*, 2007, **43**, 4872. (b) B. Roy, P. Bairi and A. K. Nandi, *Analyst*, 2011, **136**, 3605.

13 (a) X. Zhuang, D. Wang, L. Yang, P. Yu, W. Jiang and L. Mao, *Analyst*, 2013, **138**, 3046. (b) S. Chen, Y. M. Fang, Q. Xiao, J. Li, S. B. Li, H. J. Chen, J. J. Sun and H. H. Yang, *Analyst*, 2012, **137**, 2021.

14 (a) J. Deng, P. Yu, Y. Wang, L. Yang and L. Mao, *Adv. Mater.*, 2014, **26**, 6933. (b) A. Sivanesan, H. K. Ly, J. Kozuch, M. Sezer, U. Kuhlmann, A. Fischer and I. M. Wei dinger, *Chem. Commun.*, 2011, **47**, 3553.

15 (a) Y. Jiang, H. Zhao, N. Zhu, Y. Lin, P. Yu, and L. Mao, *Angew. Chem. Int. Ed.*, 2008, **47**,

8601. (b) Y. Jiang, H. Zhao, Y. Lin, N. Zhu, Y. Ma and L. Mao, *Angew. Chem. Int. Ed.*, 2010, **49**, 4800.

16 (a) Q. Qian, J. Deng, D. Wang, L. Yang, P. Yu and L. Mao, *Anal. Chem.*, 2012, **84**, 9579. (b) J. Deng, P. Yu, L. Yang, and L. Mao, *Anal. Chem.*, 2013, **85**, 2516. (c) J. Deng, Q. Jiang, Y. Wang, L. Yang, P. Yu and L. Mao, *Anal. Chem.*, 2013, **85**, 9409. (d) Y. R. Ma, H. Y. Niu, X. L. Zhang and Y. Q. Cai, *Chem. Commun.*, 2011, **47**, 12643.

17 L.Shang, C. J. Qin, L. H. Jin, L. X. Wang and S. J. Dong, *Analyst*, 2009, **134**, 1477.

18 Y. He, D. H. Liu, X. Y. He and H. Cui, *Chem. Commun.*, 2011, **47**, 10692.

19 C. H. Han, and H. B. Li, *Analyst*, 2010, **135**, 583.

20 H. Y. Niu, S. H. Wang, Z. Zhou, Y. R. Ma, X. F. Ma and Y. Q. Cai, *Anal. Chem.*, 2014, **86**, 4170.

21 W. Ha, J. Yu, R. Wang, J. Chen and Y. P. Shi, *Anal. Methods*, 2014, **6**, 5720.

22 Y. Yao, D. M. Tian and H. B. Li, *ACS. Appl. Mater. Interfaces*, 2010, **20**, 684.

23 A. J. Wang, H. M. Zhang, D. L. Zhou, R. Z. Wang and J. J. Feng, *Microchim. Acta*, 2013, **180**, 1051.

24 A. M. LopezMarzo, J. Pons, D. A. Blake and A. Merkoci, *Biosens. Bioelectron.*, 2013, **47**, 190.

25 Y. G. Guo, Y. Zhang, H. W. Shao, Z. Wang, X. F. Wang and X. Y. Jiang, *Anal. Chem.*, 2014, **86**, 8530.

26 V. Vinod Kumar and S. P. Anthony, *Sensor Actuat. B-Chem.*, 2014, **191**, 31.

27 M. Zhang, Y. Q. Liu and B. C. Ye, *Analyst*, 2012, **137**, 601.

28 H. B. Li, Y. Yao, C. P. Han and J. Y. Zhan, *Chem. Commun*., 2009, **45**, 4812.

29 J. F. Ma, J. L. Li, G. L. Zheng and J. F. Liu, *Inorg. Chem. Commun.*, 2003, **6**, 581.

30 H. B. Li, F. Y. Li, C. P. Han, Z. M. Cui, G. Y. Xie and A. Q. Zhang, *Sensor Actuat. B-Chem.*, 2010, **145**, 194.

31 R. G. Julien and N. H. V. W. Martinus, *Analyst*, 2013, **138**, 583.

32 Y. Xue, H. Zhao, Z. J. Wu, X. J. Li, Y. J. He and Z. B. Yuan, *Analyst*, 2011, **136**, 3725.

33 F. Jaliehvand, B. O. Leung and V. Mah, *Inorg. Chem.*, 2009, **48**, 5758.

34 Z. H. Shi, Q. X. Han, L. Z. Yang, H. Yang, X. L. Tang, W. Dou, Z. Q. Li, Y. G. Zhang, Y. L. Shao, L. P. Guan and W. S. Liu, *Chem. Eur. J*. 2015, 21, 290.

35 J. Ma, J. Yang, S. Li, and S. Song, *Cryst. Growth Des.*, 2005, **5**, 807-812.

36 A. Stefansson, *Environ. Sci. Technol.*, 2007, **41**, 6117-6123.

37 R. T. Bronson, D. J. Michaelis, R. D. Lamb, G. A. Husseini, P. B. Farnsworth, M. R. Linford, R. M. Izatt, J. S. Bradshaw and P. B. Savage, *Org. Lett.*, 2005, **7**, 1105.

Captions

Scheme 1 Mechanistic assay for colorimetric detection of Cd^{2+} by the SAA-AgNPs system.

Fig. 1 Response of Cd^{2+} to SAA-AgNPs. (A) UV-visible spectra and photographs (Inset) and (B) TEM images of sensor in the presence (b) and absence (a) of Cd^{2+}.

Fig. 2 FTIR spectra of pure SAA and SAA-AgNPs.

Fig. 3 Optimized experimental conditions for the SAA-AgNPs sensor. (A) Effect of the AgNPs and SAA molar ratio. (B) Plot of A_{540nm}/A_{390nm} versus time at different Cd^{2+} concentrations.

Fig. 4 Selectivity of the sensor. Blue bars represent the extinction ratio of SAA-AgNPs in the presence of Cd^{2+} and the competing species including other cations and biological species. The concentration is 0.7 μM, except that concentrations of CS, BSA and HSA are 5 ppm. Red bars are the responses from mixture of Cd^{2+} (0.7 μM) and maximum amounts of competing species. For the competing species, their concentrations are as follows: NO_2^-, Na^+, 0.7 mM; K^+, NH_4^+, Ca^{2+}, Mg^{2+}, CO_3^{2-}, and glucose, 0.07 mM; Ba^{2+}, HPO_4^{2-}, 35 μM; Hg^{2+}, Al^{3+}, Co^{2+}, Ni^{2+}, Ag^+, Zn^{2+}, SO_3^{2-}, S^{2-}, and UA , 14 μM; Cu^{2+}, Fe^{3+}, and I^-, 3.5 μM; Cr^{3+}, Mn^{2+}, and Pb^{2+}, 0.7 μM; BSA, CS, 45 ppm; HSA, 5 ppm.

Fig. 5 Photographs and UV-vis spectra of SAA-AgNPs as a function of Cd^{2+} concentrations. Arrows show the increase of Cd^{2+} concentration from 0 to 1.1 μM with 0.1 μM as the interval. Inset is the linear calibration curve between absorbance intensity ratio A_{540nm}/A_{390nm} and the concentrations of Cd^{2+}.

Table 1 Results of the Cd^{2+} Recoveries at Different Concentrations for Real Samples.

Scheme 1

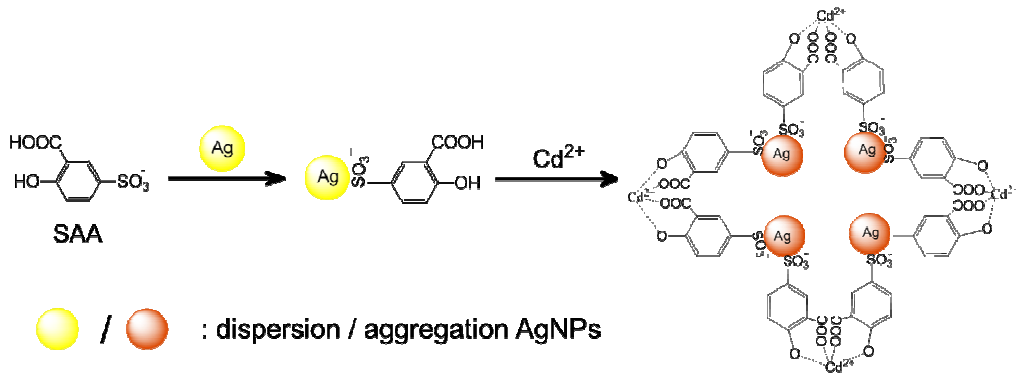

Fig. 1

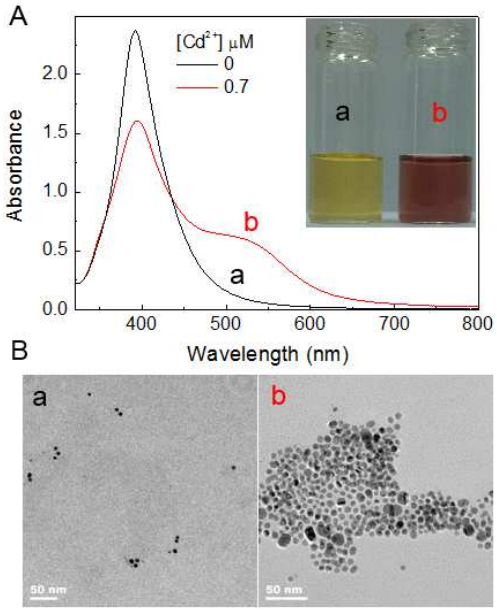

Fig. 2

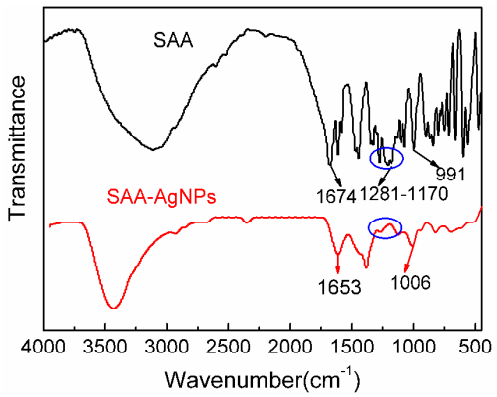

Fig. 3

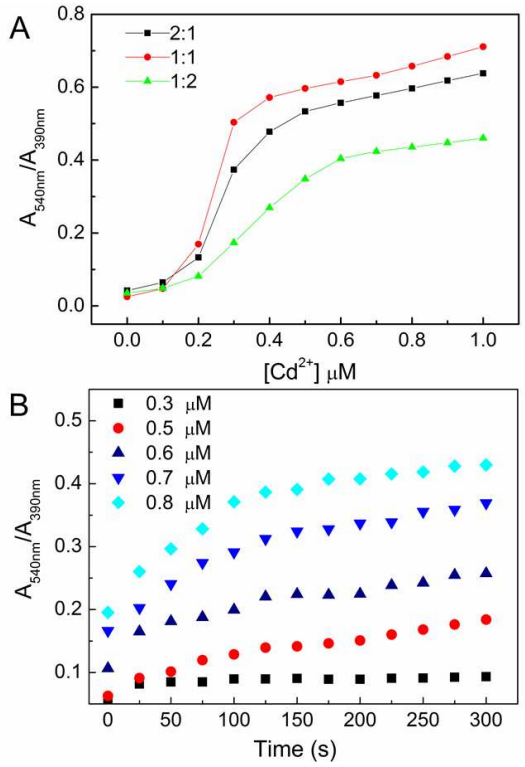

Fig. 4

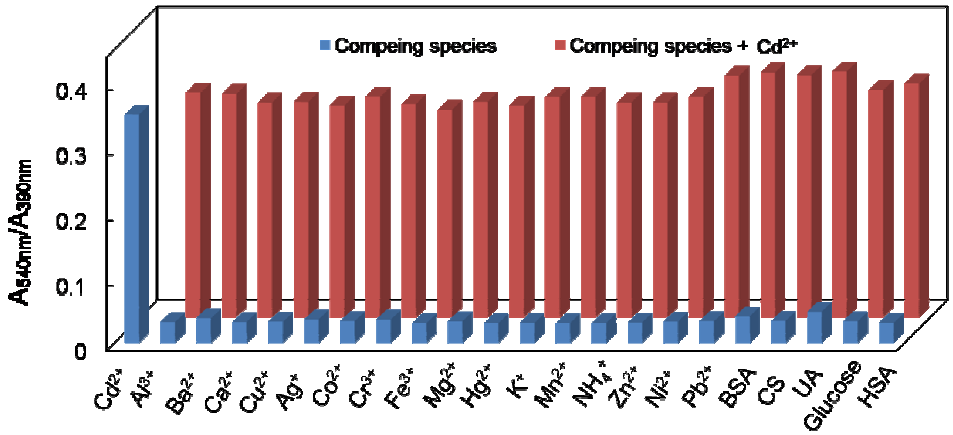

Fig. 5

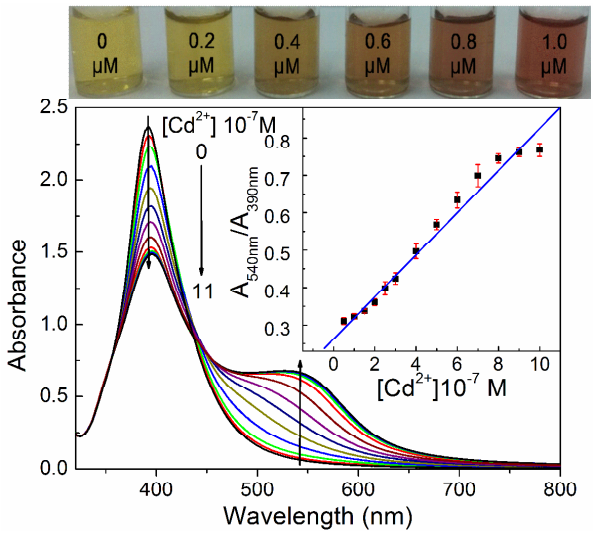

Table 1 Results of the Cd^{2+} Recoveries at Different Concentrations for Real Samples.

Sample*	Spiked (10^{-7} M)	Amount found (1.0×10^{-7} M)	Recovery (%)	RSD (%, n=3)
Serum	2.0	2.0±0.2	100	8.1
	4.0	3.6±0.3	90	7.3
	6.0	5.4±0.4	90	8.2
Urine	2.0	2.2±0.3	110	13
	4.0	3.6±0.3	90	7.7
	6.0	5.9±0.3	98	5.6
Milk	4.0	3.7±0.1	93	2.3
	8.0	7.8±0.3	98	3.9
	10.0	10.5±0.2	105	2.1
Tap water	3.0	2.9±0.06	98	2.1
	6.0	6.1±0.08	101	1.4
	8.0	8.1±0.05	100	0.6
Lake water	3.0	3.0±0.04	100	1.2
	6.0	6.2±0.2	104	3.6
	8.0	8.3±0.3	103	3.4
Spring water	3.0	3.1±0.08	103	2.7
	6.0	6.3±0.3	105	5.3
	8.0	7.9±0.05	99	0.7

*The concentration of Cd^{2+} in real samples is too low to be detected.